

Section 6

Developments in global forecast models, case studies, predictability investigations, global ensemble, monthly and seasonal forecasting

Recent progress in operational Numerical Weather Prediction at Météo-France

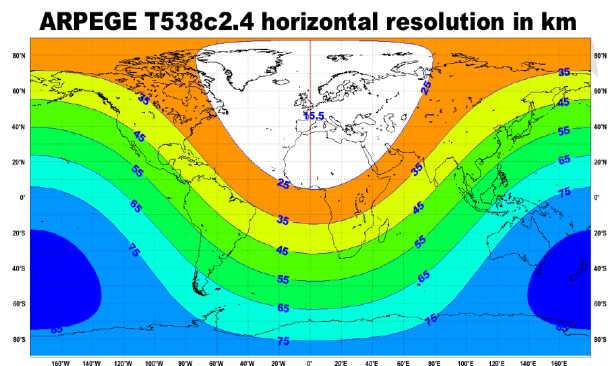
François Bouttier and collaborators

CNRM/GAME, Météo-France and CNRS
42 av Coriolis, 31057 Toulouse France
francois.bouttier@meteo.fr

Météo-France runs a comprehensive global and regional numerical weather prediction (NWP) system. The atmospheric NWP is based on the global ARPEGE, regional ALADIN and AROME models, their data assimilation systems, and an ensemble prediction system. These components stem from international (essentially European) technical and scientific cooperations: the main partners are ECMWF (www.ecmwf.int), the ALADIN consortium (www.cnrm.meteo.fr/aladin/), the HIRLAM consortium (hirlam.org) and the Méso-NH group of CNRS and the Toulouse University (mesonh.aero.obs-mip.fr/mesonh/). Increasing priority is being given to the HIRLAM cooperation on convection-scale modelling, support to the ALARO project of the ALADIN consortium, and collaboration with ECMWF on non-hydrostatic modelling and NWP software management. The resulting software is run operationally (pre-operationally, in the case of AROME), usually four times a day, on the Météo-France SX8 NEC supercomputer (used for production since Spring 2007). Additional details and updates can be found at www.cnrm.meteo.fr/gmap/.

The ARPEGE system

ARPEGE is a global, variable-resolution NWP model with a 4D-Var data assimilation. The major recent upgrade of ARPEGE is a substantial resolution increase (operational in early February 2008) and the activation of new satellite data. The new ARPEGE forecast resolution is T539L60C2.4 i.e. 15km horizontal resolution over Europe (90km over Southern Pacific); the vertical resolution has increased near the tropopause. This change (and other improvements) has substantially improved most objective forecast scores. Other changes include:



In the model and assimilation numerics:

- 4DVar increment horizontal resolution upgrade from T159 to T224
- use of vertical finite element discretisation (formulation similar to ECMWF's)
- use of a non-linear, omega multivariate balance equation in the background error covariance model
- calibration of background error covariances from an ensemble of assimilations (see below)
- variational bias correction of satellite radiances (documented elsewhere in this volume)

In the observation usage:

- assimilation of European GPS ZTD and radio-occultation GPS data from Cosmic, Champ and Grace
- assimilation of MetOp data (AMSU, MHS, HIRS, ASCAT) and ERS-2 data
- real-time monitoring of new instruments (IASI, AIRS)
- improvements to the IR radiance cloud detection scheme

In the model physics and surface assimilation:

- use of finer NESDIS SST product
- representation of soil ice melting in the soil assimilation algorithm
- revision of the evaporation of precipitation (to reduce spurious low-level divergence)
- new, efficient PDF-based algorithm to compute the sedimentation of resolved hydrometeors
- revision of the vertical diffusion in the free atmosphere

These changes have provided competitive forecast quality, particularly over Western Europe where the ARPEGE forecasts are preferred by forecasters over the IFS ones, approximately half of the time, yielding significant added value to the end forecast products.

Plans for the future include coupling 4DVar to an ensemble assimilation scheme (yielding flow-dependent background error variances, see below); assimilation of more satellite data, notably IASI and AIRS radiances,

and tropospheric microwave radiances over land and ice, thanks to a novel model of land surface emissivity (see contribution by Karbou et al in this volume); a strong increase in the horizontal density of assimilated satellite radiances; a revision to the model physics (vertical diffusion in stable boundary layers, prognostic TKE mixing, new shallow and deep subgrid convection schemes); in 2009, another upgrade will bring the ARPEGE horizontal resolution close to 10km over Europe.

The ALADIN system

The limited-area ALADIN model has inherited from most ARPEGE evolutions, except that the assimilation algorithms remains 3DVar (not 4DVar), and the horizontal resolution remains 9.5km. ALADIN-specific evolutions are:

- the assimilation of low-level temperature, humidities and winds
- configuration of a new instance of the ALADIN model and data assimilation on the South-West Indian Ocean, to aid tropical cyclone forecasting in the area
- an improved dynamical initialization system (incremental digital filters)
- a revision of the observation weights in the 3DVar analysis

It is planned to implement new instances of ALADIN in tropical areas.

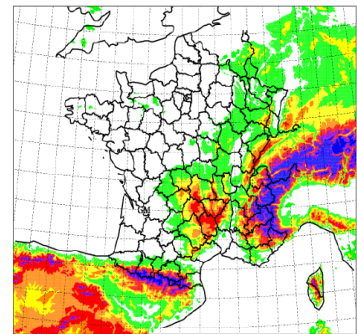
A new diagnostic version of the ALADIN 3DVar analysis system has been developed for nowcasting purposes; it draws well to the observations and has the potential to blend conventional, radar and satellite data as an aid to forecasters (e.g. for thunderstorm short-range forecast).

The AROME system

AROME is a non-hydrostatic, limited area model that inherits from the ARPEGE and ALADIN features, except for the physics (which are almost completely different and oriented towards convective scales), the NH dynamical core and special features in the data assimilation. Following intensive testing in 2007, several weaknesses of AROME have been identified and corrected, notably

- numerical performance improvements
- bug fixes in the low level physics and diagnostic computations
- a revision of the numerical diffusion
- implementation of a new subgrid shallow convection scheme (based on KFB and EDMF)
- ensemble-based model of background error covariances
- assimilation of radar data (doppler radial winds are slated for operations in 2008)

A recent AROME version improves upon ALADIN in most respects; AROME is due for operational implementation in October 2008 on a 2.5km-resolution grid that covers France and its surroundings. Preliminary tests with a 1-km resolution version of the model show encouraging performance. Current work focuses on improvements to surface assimilation, atmospheric physics tunings and the assimilation algorithm.



The ensemble systems

The Météo-France system uses an 11-member ensemble of ARPEGE 3-day forecasts at variable resolution (maximum is 24km over Europe), which serves as both a global and regional ensemble prediction system. The ARPEGE ensemble forecasts is supplied to the THORPEX/TIGGE international database since Nov 2007. A major upgrade of this system (January 2008) includes a better perturbation procedure (based on global singular and bred modes), which improves the ensemble outside the European area. Another upgrade is planned for 2008. An ensemble assimilation system has been implemented, with six members of ARPEGE assimilations similar to the deterministic ARPEGE system, except that the assimilation algorithm is 3DVar (with FGAT) and the resolution are different (globally uniform at 134km); the dispersion is driven by random perturbations of the observations. An original technique is used to derive flow-dependent analysis error variances from the ensemble of assimilations, which may then be fed into the deterministic ARPEGE 4DVar assimilation (for flow dependent observation selection and structure function) and ARPEGE ensemble prediction (for better modelling of the analysis uncertainty). The ensemble assimilation has been shown to improve the ARPEGE forecasts, it started in preoperational mode in January 2008, with operational implementation foreseen in Spring 2008.

An upgrade of the JMA Operational Global NWP Model
Kota Iwamura and Hiroto Kitagawa (*iwamura@met.kishou.go.jp*)
Japan Meteorological Agency, Tokyo, Japan

1. Introduction

The JMA operational global NWP model was upgraded to the new high resolution model on 21st Nov 2007. Introducing the new supercomputer SR11000-K1 with a peak performance of 21.5 Tflops has enabled us to improve the resolution of the model. The other major changes were in surface boundary conditions, global aerosol climatology, and the convection scheme. In this paper, we present these changes except the convection scheme (refer to "Improvement of the Cumulus Parameterization Scheme of the Operational Global NWP Model at JMA" in this volume or Nakagawa 2005), and a verification of the new model.

2. Model Resolution

Since the horizontal resolution was changed from TL319 (grid interval is about 60km) to TL959 (about 20km), and the number of horizontal grids increased from 640x320 to 1920x960, the new model can represent more detailed land/sea mask and topography. For example, the central part of Japan is expressed as a huge mountain by the old model (Figure 1, left), while the new model can resolve each major mountain (right). The better representation of topography and land/sea could improve forecasts of synoptic and sub-synoptic weather. For example, since these mountains work as a wall to prevent wind from blowing in typical winter weather conditions, new topography benefits the local weather forecasts.

The number of vertical layers increased from 40 to 60, and the pressure of the topmost level changed from 0.4hPa to 0.1hPa (Figure 2). Increased layers were given mainly to near ground surface and over the 30hPa level to improve representation of the surface boundary layer and the upper stratosphere. Furthermore, the raise of the topmost level helps to assimilate satellite observations more effectively.

3. Surface Boundary Conditions

The horizontal resolution of Sea surface temperature (SST) analysis as sea surface boundary condition was improved to 0.25 degree from 1.0 degree to bring out the detailed structure in the new high resolution forecast model. Not just the horizontal resolution was improved but the analysis method was totally revised to assimilate satellite observations with various temporal and spatial spectrums (Kurihara 2006).

In the old model, sea ice concentration (SIC) was given as boundary condition by a daily climatology interpolated from monthly statistics values. This old boundary condition was replaced with a new high resolution (0.25 degree grid) daily analysis (Cavarieli 1999). The difference between the new analysis and the old climatology is large in spring and in autumn. Figure 3 shows the difference of SIC in the Arctic Ocean between climatology (left) and analysis (right) for 21st Nov 2007. The analyzed sea ice covered more extensively over the Bering Strait and the Beaufort Sea compared to the climatology.

A snow depth and surface albedo over land are diagnosed at each time step in the land surface scheme. Since high resolution domestic observations of snow depth became available in its initial condition, the new model can predict more correctly the change in air temperature affected by snow cover.

4. Aerosol Climatology

The old model has two types of total aerosol optical depth. One is available over land, the other is over sea. Both of them were assumed to be independent of the season. The horizontal distribution of total aerosol optical depth in a new aerosol climatology is based on the actual distribution derived from the satellite data measured by MODIS and TOMS. The new model can represent regional features and seasonal changes in the distribution of aerosol. Figure 4 shows the total aerosol optical depth in May. New climatology can realistically show the dense aerosol over the deserts and the Asian dust (Aeolian dust) distributed in East Asia and the Northwest Pacific. By this upgrade, radiation flux came to be calculated more accurately in the new model.

5. Verification

Figure 5 shows the root mean square error (RMSE) of the operational forecast against the analysis for the 500hPa geopotential height in the northern hemisphere verified in Nov 2007. The new model was at an advantage of about 3-8% to the old model for every forecast time, particularly 1-2 days forecast. Improved skills were also found in other elements (temperature, wind speed, and sea level pressure), on other pressure levels, and in other regions.

Table 1 shows the improvement rate in RMSE

of trial periods which lasted 61 days in Aug/Sep 2004, and 62 days in Dec 2005 and Jan 2006. These rates are averaged over the all forecast time (1 to 9 days). The rates are positive in the most parameters.

Reference

Cavarieli, D. J., C. L. Parkinson, P. Groersen, J. C. Comiso, and H. J. Zwally, 1999: Deriving long-term time series of sea ice cover from satellite passive microwave multisensor data sets. *J. Geophys. Res.*, 104, 15,

803-15814.

Kurihara, Y., T. Sakurai and T. Kuragano, 2006: Global daily sea surface temperature analysis using data from satellite microwave radiometer, satellite infrared radiometer and in-situ observations. *Weather Bulletin, JMA*, 73, S1-S18. (in Japanese)

Nakagawa, M., 2005: Precipitation forecasts by a high resolution global model at JMA. *BMRC Research Report No.111*, 127-130.

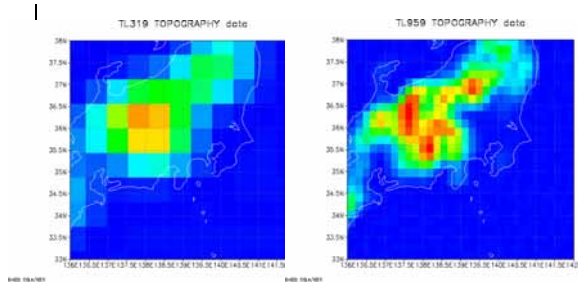


Figure 1: Model topography of the middle Japan (meters). Grid intervals are about 60km (left) and about 20km (right) in the old model and in the new model, respectively.

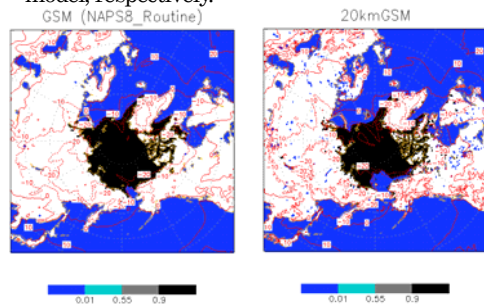


Figure 3: Distribution of sea ice concentration on 21st Nov 2007. The old model used daily climatology interpolated from original monthly values (left). The new model uses 0.25 degree daily analysis (right).

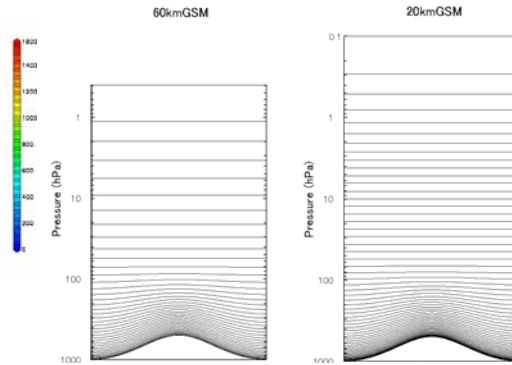


Figure 2: Profiles of vertical layers. The old model (left) and the new model (right) have 40 layers and 60 layers, respectively.

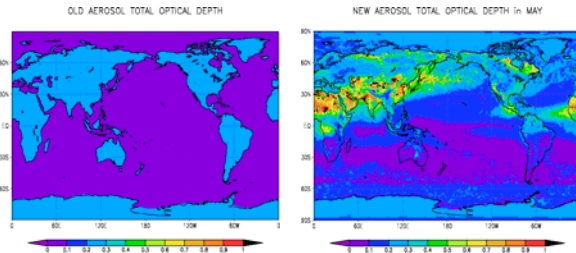


Figure 4: Distribution of total aerosol optical depth climatology in May. The old model assumes distribution which is distinguished only by land and by sea (left). The new model uses climatology derived from satellite data (right).

Table 1: Improvement rate in RMSE by the model upgrade [%]. Trial periods are 2 months in 2004 summer (top) and in 2005/6 winter (bottom). Positive values indicate an improvement of skills.

2004SM	Psea	T850	Z500	Wspd850	Wspd250
Global	+1.54	+0.41	+0.96	+0.29	+0.95
N.Hem.	-0.22	+1.52	-0.53	-0.93	+0.46
Tropics	+1.49	+1.05	-2.39	+1.32	+0.18
S.Hem.	+2.30	-0.43	+1.81	+0.51	+1.46

2006WN	Psea	T850	Z500	Wspd850	Wspd250
Global	+1.37	+1.87	+0.94	+0.10	+1.00
N.Hem.	+2.47	+2.96	+1.63	+0.33	+1.28
Tropics	+3.53	-0.77	+6.37	+1.05	+0.80
S.Hem.	-0.33	+1.06	-0.28	-0.84	+0.67

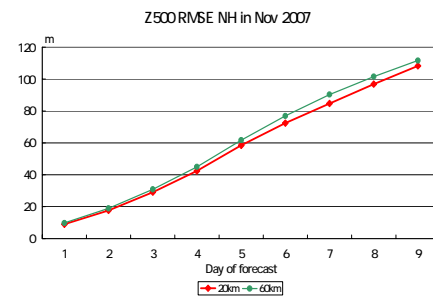


Figure 5: Root mean square error against analysis for the 500hPa geopotential height in the northern hemisphere verified in Nov 2007. Red and green lines show scores of the new model and the old model, respectively.

Trends in circulation indices extremes in reanalysis data and seasonal hindcast integrations

I.A. Kulikova, and A.V. Muraviev

Hydrometeorological Research Centre of the Russian Federation
 Bol. Predtechensky per., 11-13, 123242 Moscow, Russia
 e-mail: kulikova@mecom.ru, muravev@mecom.ru

Building on the methods and results of the previous contribution (Muravev et al, 2007), which focused on five circulation indices (Wallace, and Gutzler, 1981) calculated for daily values, the interannual variability of the circulation indices extremes within the summer and winter seasons is investigated.

Initial information is gained from the following sources: the NCEP/NCAR reanalysis for the two seasons from 1983-2002/2003, and hindcast integrations of global spectral T41L15 GCM. Integrations were performed for 90 days starting from dates 31.06 and 30.11, the SSTs were taken and preprocessed as reanalysis daily values from the same year interval. Thus, the extreme value predictability is assessed as a potential one.

A daily climate and standard deviations have been calculated on the basis of 500 hPa reanalysis and model heights for the given year period. The circulation indices were calculated as normalized daily deviations from the daily climate. The intra-seasonal index characteristics were obtained for the two data types. Examples of circulation indices for the Northern Atlantic region are given in Figure.

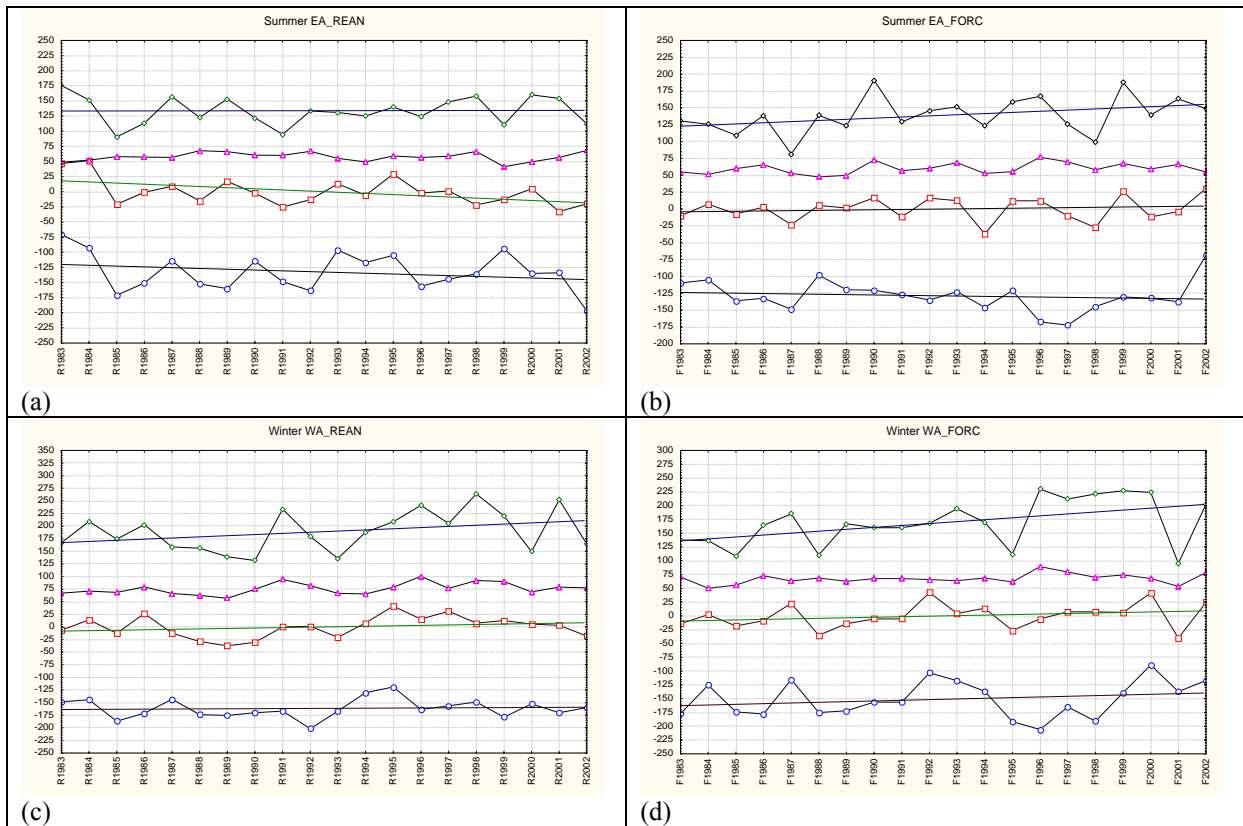


Figure. Interannual variations of characteristics of EA and WA indices ($\times 100$). The left panel contains the reanalysis data indices, the right panel carries the model data indices. Indices are as follows: summer EA (a, b), winter WA (c, d). Every panel contains, from top to bottom, curves for the following characteristics: maximum, standard deviation, mean and minimum index values within the season of the given year. Straight lines demonstrate linear trends.

The analysis of all curves yields the following conclusions. First, the variability assessed using the standard deviation is reproduced rather satisfactorily. Second, the linear trends in the mean index values are

either small or caused by sampling effects due to single outliers. Third, the minimum and maximum index values evidently point to the main variability over the year period.

Statistical significance of all calculated trends (at the rate of $60 = 2 \text{ seasons} \times 2 \text{ data types} \times 5 \text{ indices} \times 3 \text{ curves}$) is assessed with the help of the nonparametric inversions test (*Bendat, and Piersol, 1986*). The results for all circulation indices are accumulated in **Table**.

Table

Inversions number for characteristics of modeled and reanalysis index values for the 1983-2002/03 period.

Letters m, r denote the model and reanalysis data indices, respectively.

WINTER										
	EA _m	EA _r	EU _m	EU _r	PNA _m	PNA _r	WA _m	WA _r	WP _m	WP _r
Mean	97	85	89	94	93	81	68	66	78	89
Minimum	110	109	76	86	91	100	75	78	89	112
Maximum	72	86	90	103	88	84	50	63	91	86
SUMMER										
Mean	87	105	90	99	100	110	89	110	120	95
Minimum	115	83	73	72	92	102	98	84	92	89
Maximum	61	74	97	79	83	96	78	112	117	94

The three significant trends at the 95% confidence level stand out as relevant, defined by breaking out the [64,125] interval and depicted in bold in **Table**. Two of them are the maximum winter WA values for reanalysis (Fig.c), and for model data (Fig. d). The third case relates to the summer EA calculated for the model data (Fig.b). Thus, the model has reproduced the real maximum winter WA index values trend and generated a positive trend in the summer EA index not observed in reanalysis. These are the two key signals for the modeler and forecaster. Let us however highlight the fact that the no-trend hypothesis acceptance may lead to type II error, since some test values are close to critical test distribution areas.

The generation of the false trend in the summer EA index calls attention to the model blocks of the ocean-atmosphere interaction over the given geographical region of the Northern Hemisphere.

The reproduced linear trend in the maximum West-Atlantic circulation index (WA) gives a definite synoptic advantage. The trend signals of enhancement of the meridional circulation feature. This, in its turn, is expressed in the 500 hPa height trough deepening over the eastern North America and the storm-track shift towards Scandinavia. A similar shift of the cyclone activity zone towards the pole in the second part of the 20th century has been observed, for instance, in (*Hurrell et al., 2003*). The synoptic consequence of such development in the atmospheric circulation may lie in high positive temperature anomalies over the Northern Europe, as well as over the Western Siberia and Central Asia.

1. Bendat J.S., and A.G. Piersol, 1986: Random Data Analysis and Measurement Procedures. John Wiley & Sons, NewYork, Chichester, Brisbane, Toronto, Singapore.
2. Hurrell, J. W., G. Ottersen, Y. Kushnir, and M. Visbeck, 2003: An overview of the North Atlantic Oscillation. The North Atlantic Oscillation: Climatic Significance and Environment Impact, Geophys. Monogr., **134**, Amer. Geophys. Union, 1–35.
3. Muraviev A.V., I.A. Kulikova, E.N. Kruglova, 2007: Circulation indices extremes in seasonal hindcast integrations. WMO Commission for Atmospheric Sciences, Research Activities in Atmospheric and Oceanic Modelling, 20-21.
4. Wallace J.M., and D.S. Gutzler, 1981: Teleconnections in the geopotential height field during the Northern Hemisphere winter. *Monthly Weather Review*, **109**, 784-812.

Predictions of extremely low near-surface temperatures over Eastern Siberia in winter with spectral model with different resolutions

I. A. Rozinkina, E. D. Astakhova, Yu. V. Alferov, T. Ya. Ponomareva, V. I. Tsvetkov, and D. V. Blinov

Hydrometeorological Research Center of the Russian Federation, inna@mecom.ru

The near-surface temperature forecasts with the two versions of the spectral medium-range forecast model of the Hydrometeorological Center of Russia, T85L31 and T169L31, are compared. Interestingly, the appreciable progress in the model performance due to the increase in its horizontal resolution was found for some events, characterized by large horizontal scales. The simulation of extremely low temperatures in quite a uniform winter Asian anticyclone in Eastern Siberia is an example. A considerable improvement of its predictions with T169L31 is mainly due to the topography effect. The configuration of relatively low but extended relief forms is a factor strongly affecting the near-surface atmospheric cooling (down to -50 -70°C) over large regions. The orography, used in the model with coarser resolution, is too smoothed in vertical and diffused in horizontal. Low elevations are smoothed in vast regions to a plane pattern thus essentially distorting the atmospheric circulation in the lowermost model layers. And, in turn, the horizontal transfer in the lower atmospheric layers may strongly affect the near-surface temperature regime under highly stable stratification.

Fig. 1 demonstrates the skill of temperature forecasts over Eastern Siberia with T85L31 and T169L31 models for the period of very low temperatures of about -50°C . The T169L31 forecasts are much better because of the improved resolution.

Fig. 2 shows the orography used in two versions of the model. The Verkhoianskii ridge, the plateau Putorana, and relatively low, but nevertheless important, relief forms, which actually prevent the horizontal mixing of the air over inner regions of Yakutia with warmer air masses in the west and east, are too plane in the T85 orography. We managed to catch these morphometric features in the T169 orography. As a result, the spatial distribution of the near-surface air temperature was predicted better with T169L31 (see Fig. 3). The boundary layer parameterization based on the Monin-Obukhov theory (used in both versions of the model) was successful in describing the case of highly stable stratification.

Eastern Siberia is not the only place, where the above-described situation can occur. Similar events were observed in other parts of the polar regions.

Thus, the low-resolution model not only failed to describe small details of the temperature fields, but also introduced large errors in vast regions with badly described relief and was not able to “catch” some important classes of large-scale events (for example, extremely low temperatures over large regions). This conclusion is important for determining the configuration of an ensemble prediction system. The Hydrometcenter of Russia system now operates with T85L31. And the above results show that we should increase both the size of the ensemble and the resolution of the model applied. Otherwise, some large-scale important events may be missed.

The study was supported by the Russian Foundation for Basic Research (project 07-05-13607-ofi_ts).

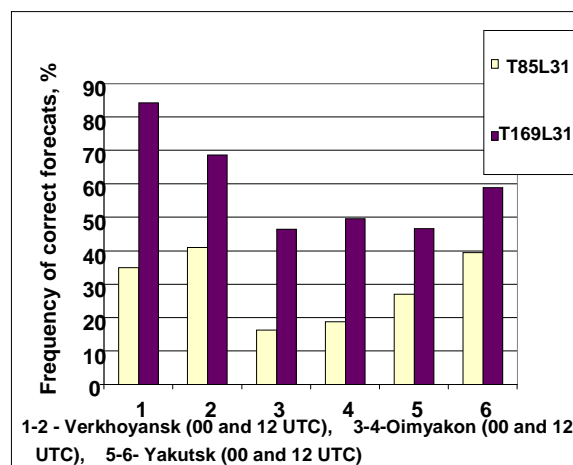


Fig.1. The skill of forecasts of 2-m temperature (the frequency of hitting the interval $T_{\text{observed}} \pm 3^{\circ}\text{C}$, averaged for lead times of 12, 24, 36, and 48 h) in December 2007 at different points in Yakutia for T85L31 and T169L31 models.

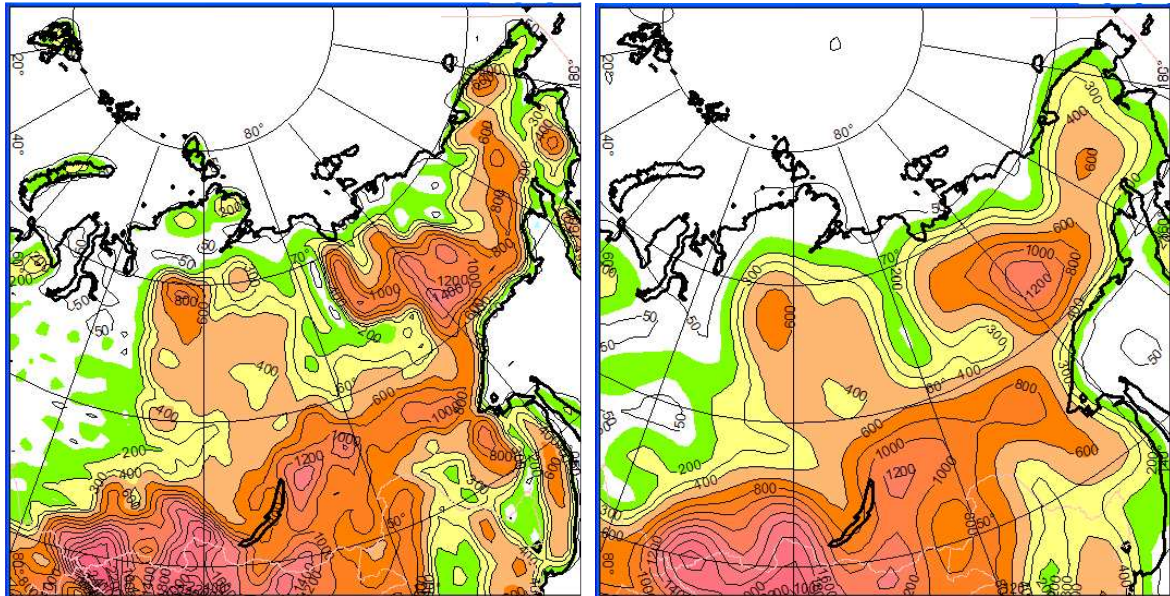


Fig.2. Model orography for T169 (left) and T85 (right). Siberia.

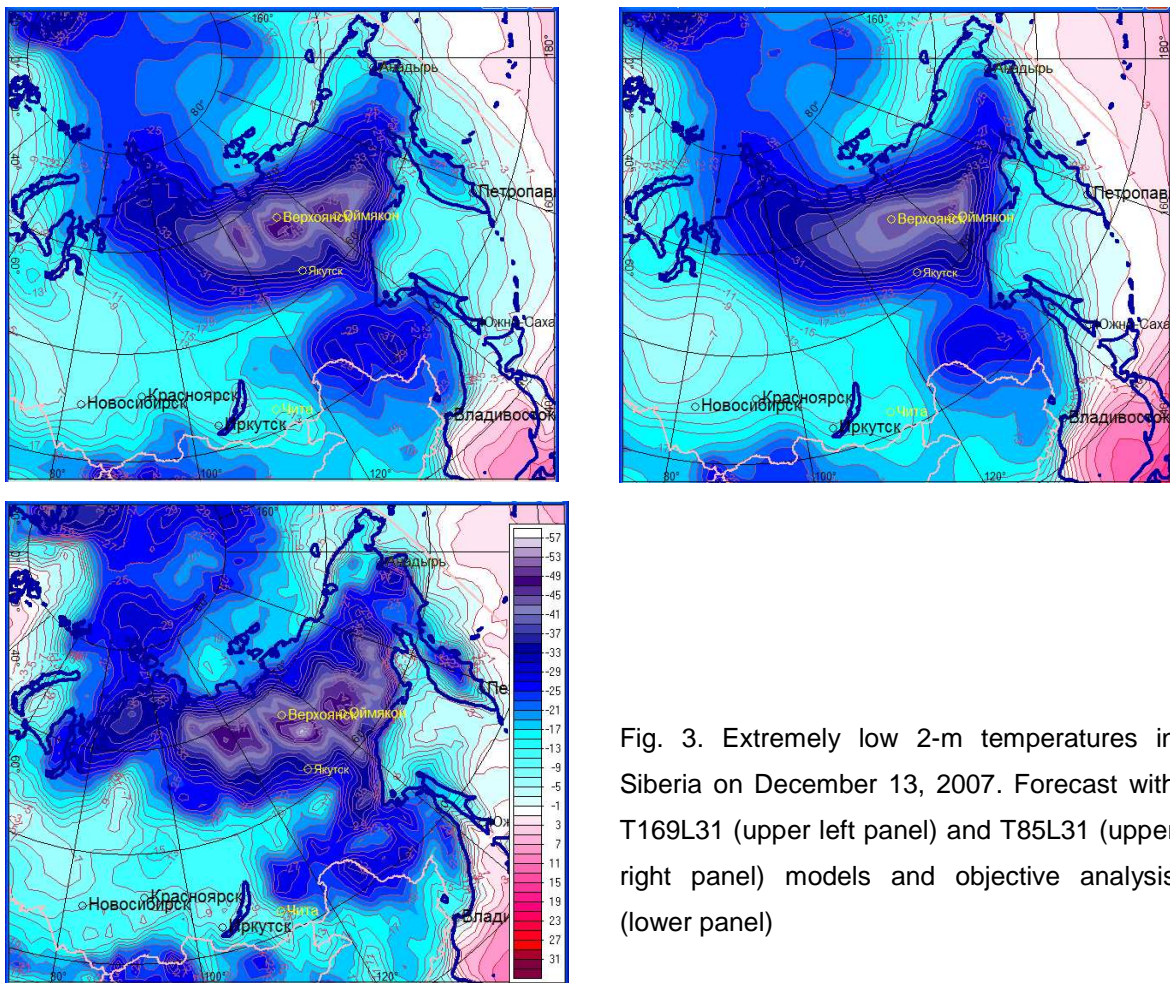


Fig. 3. Extremely low 2-m temperatures in Siberia on December 13, 2007. Forecast with T169L31 (upper left panel) and T85L31 (upper right panel) models and objective analysis (lower panel)

A new operational one-week Ensemble Prediction System at Japan Meteorological Agency

Ryota SAKAI*, Masayuki KYOUDA**, Munehiko YAMAGUCHI* and Takashi KADOWAKI*

*Numerical Prediction Division, Japan Meteorological Agency

** Climate Prediction Division, Japan Meteorological Agency

1-3-4 Otemachi, Chiyoda-ku, Tokyo 100-8122, JAPAN

(e-mail: ryouta.sakai-a@met.kishou.go.jp)

1. Introduction

Since 2001, Japan Meteorological Agency (JMA) has operated one-week Ensemble Prediction System (EPS). On November 21, 2007, JMA newly employed the Singular Vectors as an initial perturbation method, and improved the resolution of the one-week EPS. This paper reports on an outline and the performance of new one-week EPS.

2. Specifications of the new one-week EPS

The Singular Vectors (SVs) method (Buizza and Palmer, 1995) was introduced into the operational system in place of the Breeding of Growing Mode (BGM) method (Toth and Kalnay, 1993). Table 1 shows the specifications of the new initial perturbation method. A tangent linear and adjoint model used for the SVs calculation are the same as those used for the 4-dimensional variational data assimilation system (4D-VAR) in the JMA Global Spectral Model (GSM). The SVs are computed for the Northern Hemisphere (30N-90N) and the Tropics (20S-30N), separately. The moist total energy norm (Ehrendorfer, 1999) is employed for the metrics of perturbation growth. In addition to the initial SVs which are calculated from the present analysis field, the evolved SVs which are linearly integrated for optimization period up to the initial time have been also introduced into the initial perturbations. In order to construct initial perturbations with wide spatial distribution, 25 initial perturbations are obtained by combining the SVs in the respective targeted region (the Northern Hemisphere and the Tropics). After adjustment of initial perturbation amplitude using climatological variance, 50 perturbed ensemble initial fields are generated from 25 initial perturbations by adding each perturbation to analysis field positively and negatively. The analysis field for the one-week EPS ($T_L319L60$) is obtained by truncated from the high resolution Global Analysis field ($T_L959L60$).

A forecast model used in the one-week EPS is the low-resolution version of the JMA GSM (Iwamura, 2008). Table 2 shows the specifications of the old and the new one-week EPS forecast model. The horizontal and vertical resolutions are enhanced to $T_L319L60$. In addition, the deep convection scheme has been improved (Nakagawa, 2008).

Table 1 Specifications of new initial perturbation method.

	Northern Hemisphere	Tropics
Initial perturbation generator	Singular Vectors method	
Targeted region	30N - 90N	20S - 30N
Resolution of tangent-linear and adjoint model	T63L40 (1.875 deg.)	
Physical processes of inner model	* simplified-physics	** full-physics
Optimization time	48 hours	24 hours
Norm	Moist Total Energy	
Evolved SV	Used (48 hours integration)	Used (24 hours integration)
Sampling	Variance minimum method	
Amplitude of initial perturbation	12% of the climatological variance at 500hPa geopotential height	26% of the climatological variance at 850hPa temperature
Initial perturbation size	25	
Ensemble size	50 perturbed run+ 1 control run = 51 ensemble members	

* simplified-physics: Initialization, horizontal diffusion, surface turbulent diffusion and vertical turbulent diffusion.

** full-physics: In addition to the simplified-physics processes, gravity wave drag, long-wave radiation, clouds and large scale convection and cumulus convection.

Table 2 Specifications of old and new forecast model.

	Old One-week EPS	New One-week EPS
Horizontal resolution	T_L159 (1.125 deg.)	T_L319 (0.5625 deg.)
Vertical resolution (Layer)	40 (surface - 0.4hPa)	60 (surface - 0.1hPa)
Forecast time (initial time)	216 hours (12UTC)	
Time integration	3 time-level scheme (1200s)	2 time-level scheme (1200s)
Initial field	Interpolated analysis field of $T_L319L40$ into $T_L159L40$	Truncated analysis field of $T_L959L60$ into $T_L319L60$

3. Performance of the new one-week EPS

Figure 1 shows the verification result of the preliminary experimentation over the Northern Hemisphere (20N-90N) in December 2005. The anomaly correlation of the geopotential height forecast field at 500 hPa (Z500) for

the new one-week EPS is similar to that of the old one (Figure 1a). The new one-week EPS improves the relationship between the Z500 Root Mean Square Error (RMSE) of the ensemble mean and the ensemble spread around the ensemble mean which should grow at the same magnitude (Figure 1b, 1c).

Figure 2 shows the brier skill score (BSS) for the probabilistic forecast that anomaly of temperature at 850 hPa in the Eastern Asia (30N-60N, 110E-150E) is larger than 1.5 climatological standard deviation and smaller than -1.5 climatological standard deviation. The verification period is the same as Figure 1. The BSSs of the new one-week EPS are superior to that of the old one.

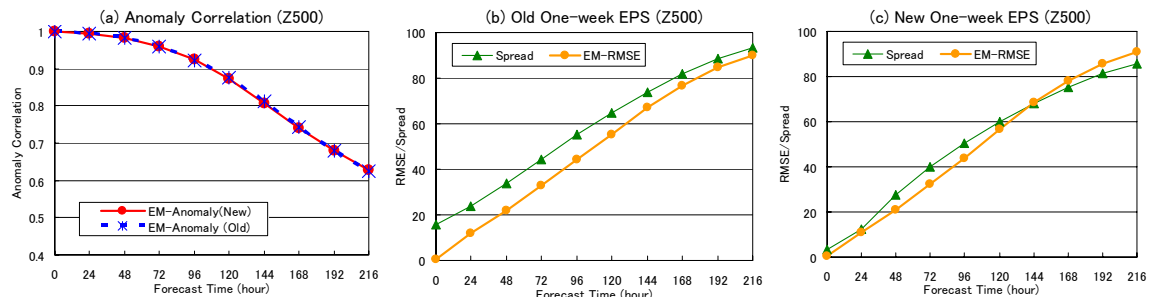


Figure 1 Verification result of the preliminary experimentation for Northern Hemisphere in December 2005. (a) Anomaly Correlation of Z500. The red line is the new EPS, the blue dashed line is the old EPS. (b) Relationship between the RMSE and the spread of Z500 for the old EPS. (c) Same as (b) but for the new EPS. In (b) and (c), the green line shows the spread around the ensemble mean, the orange line shows the ensemble mean RMSE of Z500.

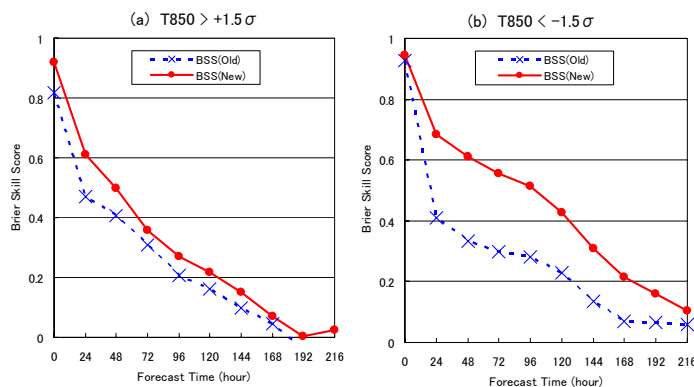


Figure 2 Probabilistic Verification of the preliminary experimentation for the East Asia in December 2005. Anomaly of T850 forecast is (a) larger than +1.5 climatological standard deviation and (b) smaller than -1.5 climatological standard deviation. The red line represents the new EPS and the blue dashed line does the old EPS.

References

- Buizza, R. and Palmer, T. N., 1995: The singular-vector structure of the atmospheric global circulation. *J. Atmos. Sci.*, **52**, 1434-1456.
- Ehrendorfer, M., R. M. Errico and K. D. Raeder, 1999: Singular-Vector perturbation growth in a primitive equation model with moist physics. *J. Atmos. Sci.*, **56**, 1627-1648.
- Iwamura, K., 2008: An upgrade of the JMA Operational Global NWP Model. Research Activities in Atmospheric and Oceanic Modelling, submitting.
- Nakagawa, M., 2008: Improvement of the Cumulus Parameterization Scheme of the Operational Global NWP Model at JMA. Research Activities in Atmospheric and Oceanic Modelling, submitting.
- Toth, Z. and E. Kalnay, 1993: Ensemble forecasting at NMC: the generation of perturbation. *Bull. Amer. Meteor. Soc.*, **74**, 2317-2330.

Typhoon Ensemble Prediction System developed at Japan Meteorological Agency

Munehiko Yamaguchi*, Ryota Sakai*, Masayuki Kyoda**, Takuya Komori*, Takashi Kadowaki*

* Numerical Prediction Division, Japan Meteorological Agency

** Climate Prediction Division, Japan Meteorological Agency

E-mail: m-yamaguchi@naps.kishou.go.jp

1. Introduction

Japan Meteorological Agency (JMA) has developed a new ensemble prediction system (EPS), the Typhoon EPS, aiming to improve both deterministic and probabilistic forecasts on tropical cyclone (TC) movements. Its full operation will start no later than the beginning of the typhoon season in 2008, following a preliminary operation which has been conducted since May 2007.

2. Specifications of the Typhoon EPS

In the Typhoon EPS, eleven initial conditions including a non-perturbed one are prepared for integration by the JMA Global Spectral Model (GSM) with horizontal spectral truncation TL319 (L representing the linear grid) and 60 vertical layers. The initial field of the non-perturbed run (control run) is made by interpolating the analysis field of the 20km (TL959) GSM which was implemented in November 2007 (Iwamura and Kitagawa 2008). The EPS focuses on TCs in the western North Pacific Ocean and the South China Sea (0-60N, 100E-180E), and runs four times a day at 0000, 0600, 1200, 1800 UTC with the forecast range of 132 hours, which covers five day forecasts. A singular vector (SV) method is employed to make initial perturbations. For the ten perturbed forecasts, five initial perturbations are created by linearly combining SVs targeted on both TCs (up to three TCs in one forecast event) and a mid-latitude region. Binding coefficients are determined so that the spatial distributions of the perturbations could widely spread. In the SV calculations targeted on TCs, moist SVs (Barkmeijer et al. 2001) are computed, on the other hand, SVs for mid-latitude are dry SVs. The norm to evaluate the growth rate of SVs is based on the moist total energy norm (Ehrendorfer et al. 1999). The evaluation time is 24 hours for both moist and dry SV calculations.

3. Performances of the Typhoon EPS

Forecast performances during the preliminary operation from May to December in 2007 are shown in this section¹. The verifications include TCs with the maximum sustained wind speed of 34kt or more. Best track data provided by RSMC Tokyo – Typhoon Center was used as analysis data. Through the verifications, we found three benefits from the EPS. First, the position errors in deterministic track forecasts are decreased. Using ensemble mean track forecasts, we obtained 40 km reduction in the position errors in the five day forecasts on average (see Fig. 1), which corresponds to the gain of about half a day lead time (not shown). Second, reliabilities become available regarding track forecasts. Referring to the amount of the ensemble spread of track forecasts, we succeeded in extracting uncertainty information on track forecasts. Based on this information, we categorized the reliability of track forecasts at each forecast time of each forecast event and assigned a reliability index, A, B, or C, to the forecast, where A, B, and C represented categories of the highest, the middle-level, and the lowest reliability, respectively, (see Fig. 2) and the frequency of each category was set to 40%, 40%, and 20%. As shown in Fig.3, when gathering all forecasts judged as A, it proved that the average position errors were considerably smaller than those of all track forecasts shown in Fig.1. On the contrary, when gathering forecasts judged as C, the average position errors were larger than the average position errors of all forecasts. This result reflects the fact that there is a strong spread-skill relationship in the track forecasts by the EPS. Last, alternative track scenarios to an ensemble mean track become available. Because of the possibility that an ensemble mean track forecast may miss a true TC movement, identifying all possible track scenarios is important. More importantly, one of the scenarios should have smaller errors than those of an ensemble mean track, particularly in cases where it had quite large errors. Figure 4 shows the comparison of position errors of three day forecasts (12 UTC initials only); the blue bars represent the position errors by ensemble mean track forecasts, which are sorted in ascending order, and the red bars represent the corresponding errors by a cluster whose errors proved to be the lowest among several scenarios which are identified using a cluster analysis method. In this method, we combined the Typhoon EPS (11 members) with the One-week EPS (51 members, Sakai et

¹. Though the specifications of the preliminary operation are a little different from those of the full operation, we confirmed through some experiments that the differences of the performances are small.

al. 2008) at JMA and made an ensemble with 62 members so as to capture as many scenarios as possible and reduce the risk of missing. As Fig. 4 shows, it is found that one of some scenarios could represent a true TC movement rather than an ensemble mean forecast in cases where it had more than 500 km position errors.

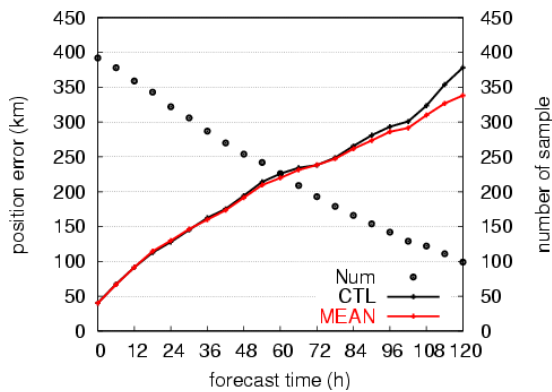


Fig. 1. Position errors of ensemble mean track forecasts (red) up to five days compared with those of track forecasts by control run (black). Y-axis on the left represents the position errors (km). Dots mean the number of sample at each forecast time's verification (see y-axis on the right).

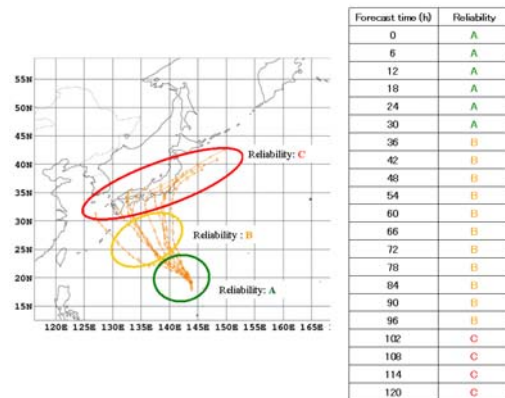


Fig. 2. An example of applications of the Typhoon EPS. A, B and C on the figure represent reliabilities on track forecasts, where A means the highest reliability. Each index is given based on the ensemble spread of track positions at each forecast time.

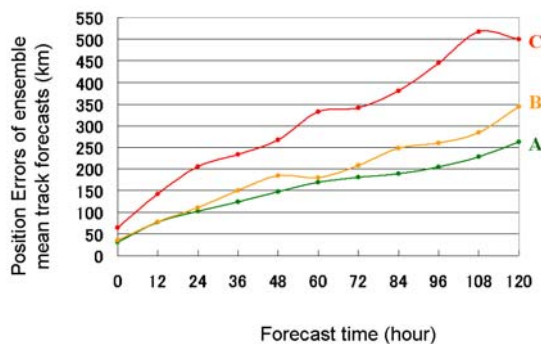


Fig. 3. Position errors of ensemble mean track forecasts of each reliability; A, B and C, where A represents the highest reliability. Green line shows the position errors of track forecasts with the highest reliability; A. Yellow and red lines correspond to the results of reliability B and C, respectively.

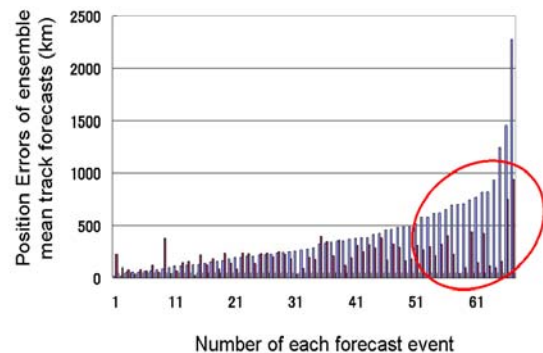


Fig. 4. Comparison of position errors of three day forecasts (12 UTC initials only). Blue bars represent the position errors by ensemble mean track forecasts, which are sorted in ascending order, and red bars represent the corresponding errors by a cluster whose errors proved to be the lowest among several scenarios. X-axis shows a number of each forecast event and y-axis does position errors (km).

Reference

Barkmeijer, J., Buizza, R., Palmer, T. N., Puri, K. and Mahfouf, J. F., 2001: Tropical singular vectors computed with linearized diabatic physics. *Quart. J. Roy. Meteor. Soc.*, **127**, 685-708.
 Ehrendorfer, M., R. M. Errico and K. D. Raeder, 1999: Singular-vector perturbation growth in a primitive equation model with moist physics. *J. Atmos. Sci.*, **56**, 1627-1648.
 Iwamura, K. and H. Kitagawa, 2008: An upgrade of the JMA Operational Global NWP Model. *CAS/JSC WGNE Research Activities in Atmospheric and Oceanic Modelling*. (submitted)
 Sakai, R., M. Kyoda, M. Yamaguchi and T. Kadowaki, 2008: A new operational One-week Ensemble Prediction System at Japan Meteorological Agency. *CAS/JSC WGNE Research Activities in Atmospheric and Oceanic Modelling*. (submitted)